PHYSICAL REVIEW B VOLUME 33, NUMBER 10 15 MAY 1986

Theory of the lateral surface magnetoplasmon in a semiconductor superlattice

Ji-Wei Wu, P. Hawrylak, Gunnar Eliasson, and J. J. Quinn
Brown University, Providence, Rhode Island 02912
(Received 9 December 1985)

We study in detail the properties of the recently predicted magnetoplasmon excitations localized near the lateral surface of a semi-infinite superlattice. The dispersion relation of these surface modes is obtained both by a simple approximate method and by a numerical technique capable of arbitrary precision. Possible experimental observation of the surface excitation spectrum is discussed.

I. INTRODUCTION

During the past few years the spectrum of the collective excitations of semiconductor superlattices has received a considerable amount of attention both from a theoretical as well as from an experimental point of view.[1–14] Both intra- and intersubband excitations of infinite superlattices have been investigated. For the former, the superlattice can be treated as a periodic array of two-dimensional electron-gas (2D EG) layers. For the latter, the subband energies and wave functions of the multiple-quantum-well structure must be accounted for. Theoretical predictions on the intrasubband bulk excitation spectrum[2–4] have been confirmed by the inelastic light scattering experiment of Olego *et al.*[5] A new type of intrasubband surface mode, with the remarkable property of freedom from Landau damping, has been proposed by Giuliani and Quinn for a surface parallel to the layers of a semi-infinite superlattice.[12]

In a recent report,[15] we analyzed intrasubband surface modes of the lateral surfaces (i.e., the surfaces perpendicular to the layers of the superlattice) of such a system. The surface collective excitations associated with these surfaces (coupled edge plasmons of constituent two-dimensional electron layers) were predicted and their dispersion was determined approximately. The dispersion of these edge plasma modes (and magnetoplasma modes) depends on the components of the wave vector in the two principal directions of propagation parallel to the lateral surface plane, q along the edges of the conducting planes and p along the superlattice axis, and normal to the conducting planes. For fixed p, these edge modes display linear behavior as a function of q in the long-wavelength limit. The Bloch condition in the direction parallel to the superlattice axis gives rise to a band of excitation spectrum for all possible values of $0<p<\pi/d$. Imposing a static magnetic field parallel to the surface has the effect of separating the surface excitation spectrum from the bulk spectrum. This property should be very helpful in identifying these surface modes experimentally.

In this paper we provide a detailed discussion of these lateral surface magnetoplasmon excitations. Besides the approximate solution we developed earlier, a numerically exact solution is obtained by expanding the potential in terms of a complete set of orthogonal functions and transforming the integral equation into a matrix equation of infinite order. This method, when combined with the mirror-image technique, can be used to solve the problem in the more general and realistic situation in which the background dielectric constants on the opposite sides of the surface are different.

The remainder of this paper is organized as follows. In Sec. II we present the derivation of an integral equation for the electrostatic potential of the system. In Sec. III we review the approximate solution to the integral equation. In Sec. IV the integral equation is transformed into a matrix equation and the dispersion relation is obtained by solving the secular equation numerically. In Sec. V we generalize the solution to the problem in which different background dielectric constants are present on opposite sides of the interface by employing the mirror-image technique. A discussion on the results and possible experiments is given in Sec. VI.

II. POTENTIAL EQUATION OF THE SYSTEM OF A LATERAL SEMI-INFINITE SUPERLATTICE

In our model of a semi-infinite superlattice the space $x<0$ is occupied by a semiconductor of background dielectric constant ϵ_s, while the space $x>0$ is filled by an insulator of dielectric constant ϵ_0. The semiconductor contains an infinite array of conducting planes at $z=na$ with $n=0,\pm1,\ldots$. Each plane contains n_s electrons per unit area of mass m, and the entire semiconductor contains a uniform neutralizing positive charge background. We restrict our consideration to the electrostatic limit where the velocity of light can be taken to be infinite, and the electric field $E=-\nabla\phi$ can be expressed as the gradient of a potential. We consider the equilibrium charge density $n_s\sum\delta(z-la)\Theta(-x)$ to be perturbed by a fluctuation $\delta n(\mathbf{r},t)$. The system is shown schematically in Fig. 1. The 2D EG layers are parallel to the xy plane. A static magnetic field $\mathbf{B}$ is in the z direction. For waves localized near the surface $x=0$, the density fluctuation and the corresponding *ac* potential are of the form

$$\delta n(\mathbf{r},t)=\sum_l n_l(x)\delta(z-la)\exp(iqy-i\omega t)\ , \qquad (2.1)$$

$$\phi(\mathbf{r},t)=\phi(x,z)\exp(iqy-i\omega t)\ . \qquad (2.2)$$

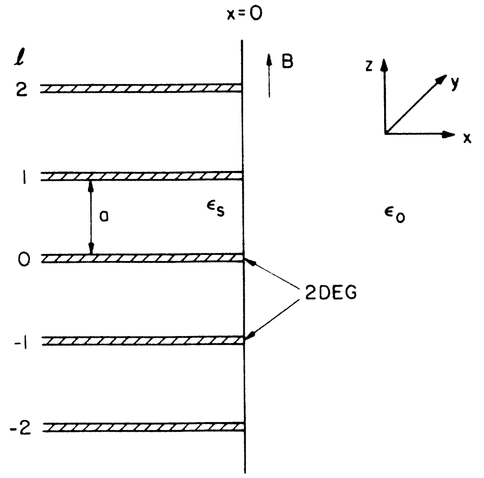

FIG. 1. Schematic drawing of a semi-infinite superlattice with background dielectric constant ϵ_s occupying the region $x<0$. 2DEG layers are parallel to the xy plane with equal space a. Each layer has an equilibrium charge distribution n_s per unit area. A static magnetic field lies along the z direction which is parallel to the interface and normal to the 2DEG layers.

In this section we derive an integral equation for $\phi(x,z)$, which is solved in subsequent sections. The dispersion relation is determined from the conditions for the existence of a nontrivial self-consistent solution.

We start from the following three basic equations in electrodynamics. They are Poisson's equation,

$$\nabla\cdot[\epsilon(\mathbf{r})\mathbf{E}(\mathbf{r})]=4\pi\delta n(\mathbf{r})\ ; \tag{2.3}$$

the equation of continuity,

$$\nabla\cdot\mathbf{J}=i\omega\delta n(\mathbf{r})\ ; \tag{2.4}$$

and the constitutive equation,

$$\mathbf{j}_l(x)=\overleftrightarrow{\sigma}\cdot\mathbf{E}(x)\ . \tag{2.5}$$

Here we have written the current density as

$$\mathbf{J}(\mathbf{r},t)=\sum_l \mathbf{j}_l(x)\delta(z-la)\exp(iqy-i\omega t)\ .$$

$\overleftrightarrow{\sigma}(\omega)$ is the local conductivity tensor of the 2DEG, $\mathbf{E}_l(x)$ is the electric field at $z=la$, and the background dielectric function is

$$\epsilon(x)=\epsilon_s+(\epsilon_0-\epsilon_s)\Theta(x)\ . \tag{2.6}$$

The equation for $\phi(x,z)$ is obtained by taking the Fourier transform of Eq. (2.3) and using (2.2),

$$\epsilon(x)\phi(x,z)=4\pi\int_{-\infty}^{0}dx'\int_{-\infty}^{\infty}dz' I_q(x-x',z-z')\delta n(x',z') +(\epsilon_s-\epsilon_0)\frac{\partial}{\partial x}\int_{-\infty}^{\infty}dz' I_q(x,z-z')\phi(x'0,z')\ , \tag{2.7}$$

where we have defined the function

$$I_q(x,z)=K_0(q(x^2+z^2)^{1/2})/2\pi \tag{2.8}$$

and K_0 is the modified Bessel function.

For a superlattice with periodicity a in the z direction, the density fluctuation on the lth layer can be related to that on the zeroth layer by the Bloch condition,[3]

$$n_l(x)=e^{ipla}n_0(x)\ . \tag{2.9}$$

The entire spectrum of dispersion is defined by values of p satisfying $0\le p\le\pi/a$. Setting $z=0$ and using the notation of $\phi(x)\equiv\phi(x,z=0)$ allows Eq. (2.7) to be expressed in the form

$$\epsilon(x)\phi(x)=4\pi\int_{-\infty}^{0}dx' L_{\mathbf{q}}(x-x')n_0(x') +(\epsilon_s-\epsilon_0)\frac{\partial}{\partial x}\int_{-\infty}^{\infty}dz' I_q(x,z')\phi(0,z')\ . \tag{2.10}$$

In the first term on the right-hand side, the kernel inside the integral is

$$L_{\mathbf{q}}(x)=\sum_{l=-\infty}^{\infty}e^{ipla}I_q(x,la) =\int\frac{dk_x}{4\pi}e^{ik_x x}(k_x^2+q^2)^{-1/2}S[(q^2+k_x^2)^{1/2},p]\ . \tag{2.11}$$

The vector notation $\mathbf{q}$ means (q,p) in our discussion, and

$$S(q,p)=\frac{\sinh(qa)}{\cosh(qa)-\cos(pa)} \tag{2.12}$$

is the structure factor. In the limit of $qa\to\infty$, we have

$$L_q(x)=K_0(q\,|x|\,)/2\pi\ , \tag{2.13}$$

which gives the correct form for the single-layer problem.[16]

Equations (2.3) and (2.4) relate the density fluctuation $n_0(x)$ to $\phi(x)$ by the equation

$$n_0(x)=\Theta(-x)(\sigma_{xx}/i\omega)\left[q^2-\frac{\partial^2}{\partial x^2}\right]\phi(x) -\frac{1}{i\omega}j_{0,x}(x=0^-)\delta(x)\ . \tag{2.14}$$

Here we have written explicitly the two terms in $n_0(x)$; the first term is the regular contribution from $x<0$, while the δ-function term indicates the singularity of charge density at $x=0$ due to the discontinuity of the current. The integral equation becomes

$$\epsilon(x)\phi(x)=\frac{4\pi\sigma_{xx}}{i\omega}\int_{-\infty}^{\infty}dx' L_{\mathbf{q}}(x-x')\left[q^2-\frac{\partial^2}{\partial x^2}\right]\phi(x') -\frac{4\pi}{i\omega}j_{0,x}(0^-)L_{\mathbf{q}}(x) +(\epsilon_s-\epsilon_0)\frac{\partial}{\partial x}\int_{-\infty}^{\infty}dz\, I_q(x,z)\phi(0,z)\ . \tag{2.15}$$

The conductivity tensor is determined from the simple Drude model; by combining the equation of motion for an electron

$$m\frac{d\mathbf{v}}{dt}=e\mathbf{E}+\frac{e}{c}\mathbf{v}\times\mathbf{B} \tag{2.16}$$

with the expression for current

$$j_0(x)=\Theta(-x)en_s\mathbf{v}(x)\ , \tag{2.17}$$

it is straightforward to show that

$$\sigma_{xx}(\omega)=\frac{in_se^2\omega}{m(\omega^2-\omega_c^2)}\ ,\qquad \sigma_{xy}(\omega)=i\frac{\omega_c}{\omega}\sigma_{xx}(\omega)\ , \tag{2.18}$$

and

$$j_{0,x}(0^-)=\sigma_{xx}\left[\phi'(0^-)-q\frac{\omega_c}{\omega}\phi(0^-)\right]\ , \tag{2.19}$$

where $\omega_c=eB/mc$ is the cyclotron frequency, and $\phi'(0^-)=[\partial\phi(x)/\partial x]_{x=0^-}$.

In the remainder of this paper we solve the potential equation (2.15) by different methods. The dispersion relation of edge plasmon modes is obtained from the requirement for the existence of a nontrivial surface wave solution. To make the formalism simple, we first give the derivation under the assumption of $\epsilon_0=\epsilon_s$ in Secs. III and IV, while the general situation of $\epsilon_0\neq\epsilon_s$ is treated in Sec. V.

III. SIMPLE APPROXIMATE SOLUTION

In this section we solve the potential equation by using an approximate kernel $L'_q(x)$ instead of the exact one $L_q(x)$ in Eq. (2.11). A numerically exact solution will be given in the next section. The reason for doing this is that the approximation gives qualitatively correct results in a simple way, and the dispersion relation can be easily computed for given parameters. This should be useful in searching for the collective modes predicted in this paper.

Under the assumption $\epsilon_0=\epsilon_s$ the last term on the right-hand side of Eq. (2.15) vanishes. The potential satisfies the approximate equation

$$\phi(x)=\frac{4\pi\sigma_{xx}}{i\omega\epsilon_s}\int_{-\infty}^{0}dx'L'_q(x-x')\left[q^2-\frac{\partial^2}{\partial x^2}\right]\phi(x')-\frac{4\pi}{i\omega\epsilon_s}j_{0,x}(0^-)L'_q(x)\ . \tag{3.1}$$

We choose the approximate kernel $L'_q(x)$ in Eq. (3.1) to be of the form

$$L'_q(x)=\frac{\alpha(q)}{2\sqrt{2}}e^{-\sqrt{2}\alpha q|x|}\ , \tag{3.2}$$

where the parameter α is

$$\alpha(q)=\left[1-\frac{qa}{\sinh(qa)}\left[\frac{1-\cosh(qa)\cos(pa)}{\cosh(qa)-\cos(pa)}\right]\right]^{-1/2}. \tag{3.3}$$

This choice makes $L'_q(x)$ have the same area and second moment as the exact kernel in Eq. (2.11). In the limit of $qa\to\infty$, Eq. (3.2) reduces to the approximate kernel used by Mast *et al.*[16] for the single-layer problem. Our solution reduces to their approximate result in this limit. In the opposite limit $qa\to 0$ and $pa=0$, we would have $\alpha=1/\sqrt{2}$ and $L_q(x)=\frac{1}{4}e^{-q|x|}$. The integral equation (3.1) can be solved by using the Wiener-Hopf technique;[17] the solution in the region $x<0$ turns out to be

$$\phi(x<0)=\tfrac{1}{2}\phi(0^-)\left[\left[1-(\sqrt{2}+b_1)\frac{q}{\gamma}\right]e^{\gamma x}+\left[1+(\sqrt{2}+b_1)\frac{q}{\gamma}\right]e^{-\gamma x}\right]\ , \tag{3.4}$$

where

$$\gamma=q(2+b_2)^{1/2},\quad b=\left[\sqrt{2}\pm\frac{\omega_c}{\omega}\right]b_2\ ,$$

and

$$b_2=2\omega_p^2/(\omega^2-\omega_c^2-\omega_p^2)\ .$$

The condition for a surface wave is that the coefficient of the exponentially growing term must vanish. This gives the dispersion relation of the edge magnetoplasmon

$$(2\alpha^2+1)\omega^2\pm2\sqrt{2}\alpha\omega\omega_c-\alpha^2Sqa\,\Omega_p^2/\epsilon_s=0\ , \tag{3.5}$$

where $\Omega_p^2=4\pi n_se^2/ma$ is the three-dimensional plasmon frequency of a system with electron density n_s/a. The plus and minus signs in the equation correspond to waves propagating to the right- or left-hand side (in the $+y$ or $-y$ direction).

In the absence of the static magnetic field, the modes propagating in opposite directions are degenerate for given q and p. In the general case where $\omega_c\neq0$, the resulting degeneracy is removed by the presence of a magnetic field.

In the limit $qa\to0$ and $pa=0$, Eq. (3.5) reduces to

$$\omega(\omega\pm\omega_c)=\Omega_p^2/2\epsilon_s\ , \tag{3.6}$$

which is the well-known dispersion relation of a surface magnetoplasmon of a homogeneous medium of the same average electron density.[18] This indicates that our approximate dispersion relation would reach the exact solution for small values of qa. For $qa\to\infty$, the dispersion relation reduces to

$$3\omega^2+2\sqrt{2}\omega\omega_c-2\omega_p^2=0\ , \tag{3.7}$$

where $\omega_p=2\pi n_se^2q/m$ is the square of the frequency of a two-dimensional plasmon of wave vector q. Equation (3.7) was first derived by Mast *et al.*[16] in order to explain their experimental data on the resonances of a single-layer classical two-dimensional electron gas at a liquid-helium surface.

Figure 2 gives a plot of ω versus qa for the dispersion relation in the absence of a magnetic field [$\omega_c=0$ in Eq. (3.5)]. The waves propagating in opposite y directions are degenerate. For each value of $p\neq0$, the dispersion is linear for $qa\ll1$. The acoustical nature of these surface waves might be useful for surface wave devices. Figure 3 gives a plot of the dispersion for $\omega_c=2\Omega_p/(\epsilon_s)^{1/2}$. There

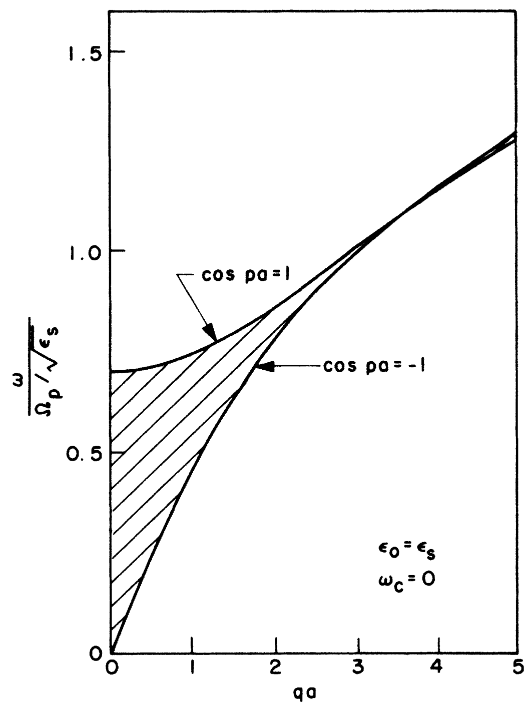

FIG. 2. Dispersion of lateral surface plasmon modes in the absence of a static magnetic field. Waves propagating toward plus and minus y directions are degenerate. The background dielectric constants on both sides of the surface are assumed to be the same.

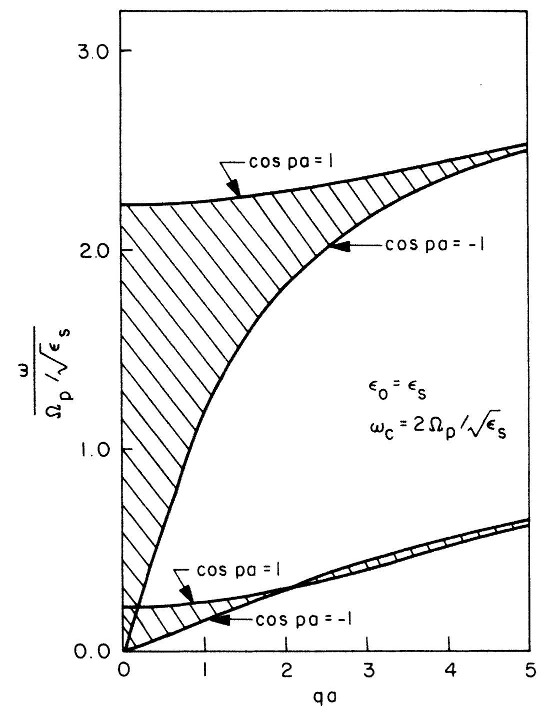

FIG. 3. Dispersion of lateral surface plasmon modes in a superlattice with a static magnetic field pointing in the z direction. The corresponding cyclotron frequency is $\omega_c = 2\Omega_p/(\epsilon_s)^{1/2}$. The upper band indicates waves propagating toward plus y direction, while the lower band indicates waves toward minus y direction.

are two bands of surface modes corresponding to opposite directions of propagation along the y axis. The band propagating toward the positive y direction [minus sign in Eq. (3.5)] extends above ω_c, while the other one is pressed much lower than $\Omega_p/(\epsilon_s)^{1/2}$. For each value of pa, the phase velocity of the wave propagating in the y direction (along the layer) is defined by

$$v_s(p) = \lim_{qa \to 0} \omega(q,p)/q \ . \tag{3.8}$$

The minimum speed is determined by taking $pa = \pi$. Equation (3.5) gives for the minimum phase velocity of the edge plasmons,

$$V_s(q, pa=\pi) = \frac{a}{4}[\pm\sqrt{3}\omega_c + (3\omega_c^2 + 9\Omega_p^2/\epsilon_s)^{1/2}] \ . \tag{3.9}$$

If we take $\Omega_p/(\epsilon_s)^{1/2} \approx 10^{13}$ sec^{-1}, and $a = 500$ Å, the phase velocity could be as high as 4×10^7 cm/sec in the absence of a magnetic field. However, this quantity would be reduced by a factor of 10 or more by the introduction of a magnetic field with $\omega_c > \Omega_p/(\epsilon_s)^{1/2}$. The magnetic field also has the effect of separating the lower band in Fig. 3 from the spectrum of bulk excitations. It is much more favorable to perform experiments in the presence of a magnetic field which can be varied over a broad range of values.

IV. NUMERICAL SOLUTION OF THE DISPERSION RELATION

By keeping the exact kernel $L_{\mathbf{q}}(x)$ in the integral equation (3.1), the potential equation is

$$\phi(x) = \frac{4\pi\sigma_{xx}}{i\omega\epsilon_s} \int_{-\infty}^{0} dx' L_{\mathbf{q}}(x-x') \left[q^2 - \frac{\partial^2}{\partial(x')^2} \right] \phi(x') - \frac{4\pi}{i\omega\epsilon_s} j_x(0^-) L_{\mathbf{q}}(x) \ . \tag{4.1}$$

In the region of $x<0$, we expand both sides of the equation in terms of Laguerre polynomials of the following form:

$$\phi(x<0) = \exp(qx) \sum_{n=0}^{\infty} L_n(-2qx)\alpha_n \ . \tag{4.2}$$

Because of the orthonormality of this expansion,

$$\alpha_n = 2q \int_{-\infty}^{0} dx \exp(qx) L_n(-2qx)\phi(x) \ . \tag{4.3}$$

Equation (4.1) is readily transformed into a matrix equation for the expansion coefficients

$$\alpha_n = \frac{4\pi\sigma_{xx}}{i\omega\epsilon_s} \sum_{n'=0}^{\infty} \alpha_{n'} [J_{nn'} + (2n'+1 \mp \omega_c/\omega) I_n] \ , \tag{4.4}$$

where we have defined two integrals

$$J_{nn'}=2q\int_{-\infty}^{0}dx\,\exp(qx)L_n(-2qx)\int_{-\infty}^{0}dx'L_q(x-x')\left[q^2-\frac{\partial^2}{\partial(x')^2}\right][\exp(qx')L_{n'}(-2qx')] \tag{4.5}$$

and

$$I_n=2q^2\int_{-\infty}^{0}dx\,\exp(qx)L_n(-2qx)L_q(x)\ . \tag{4.6}$$

Notice that we have used the identities

$$\phi(x=0^-)=\sum_{n=0}^{\infty}\alpha_n \tag{4.7}$$

and

$$\phi'(x=0^-)=\sum_{n=0}^{\infty}\alpha_n(2n+1) \tag{4.8}$$

from the definition of Eq. (4.2).

The integrals $J_{nn'}$ and I_n can be evaluated in closed form for $L_q(x)$ given in Eq. (2.11). The matrix equation (4.4) can be written

$$\alpha_n=D\sum_{n'=0}^{\infty}\alpha_{n'}[S_{nn'}+(1\mp\omega_c/\omega)F_n]\ , \tag{4.9}$$

where the symbols D, $S_{nn'}$, and F_n are given by

$$D=\frac{4\pi\sigma_{xx}}{i\omega\epsilon_s a}=\frac{\Omega_p^2}{(\omega^2-\omega_c^2)\epsilon_s}\ , \tag{4.10}$$

$$S_{nn'}=\sum_{m=-\infty}\left[\left[\frac{\gamma-1}{\gamma+1}\right]^{|n-n'|}-\left[\frac{\gamma-1}{\gamma+1}\right]^{n}\right]\Big/\gamma\ , \tag{4.11}$$

$$F_n=\sum_{m=-\infty}\frac{(\gamma-1)^n}{\gamma(\gamma+1)^{n+1}}\ . \tag{4.12}$$

In these equations $\gamma(m)$ stands for

$$\gamma(m)=\left[1+\left[\frac{pa+2m\pi}{qa}\right]^2\right]^{1/2}\ . \tag{4.13}$$

The series $S_{nn'}$ and F_n converge rapidly for finite qa and $0<pa<\pi$. The dispersion relation of the lateral surface magnetoplasmon is determined from the zero of the following determinant of infinite order:

$$0=\det[\delta_{nn'}-D(S_{nn'}+(1\mp\omega_c/\omega)F_n)]\ . \tag{4.14}$$

We have computed this determinant by truncating the expansion at a finite order N, and found that its roots converge rapidly with increasing N toward their $N=\infty$ limits. Within the range of our computation, the error is negligible for $N>10$. Therefore, Eq. (4.14) gives an accurate solution to the dispersion.

Figures 4 and 5 plot the dispersion relation from the numerical solution of Eq. (4.14) for the same parameters as in Figs. 2 and 3. Comparing Fig. 4 to Fig. 2, we see that solution Eq. (3.5) gives a good approximation to the dispersion at $\omega_c=0$ for values of qa not too large. In the region of $qa\gg 1$ the approximation becomes worse and incorrectly predicts the crossing of the two lines of $\cos(pa)=\pm 1$. In the presence of a magnetic field with $\omega_c=2\Omega_p/(\epsilon_s)^{1/2}$, Eq. (4.14) gives two bands corresponding to propagation of waves in the $+y$ or $-y$ direction. The lower band exhibits acoustical behavior in the long-wavelength limit for $pa\neq 0$, while the upper band is above ω_c. This shows that the approximate solution is qualitatively correct only for the lower band. Notice that both Eqs. (4.5) and (4.14) approach the exact result of $\omega(\omega\pm\omega_c)=\Omega_p^2/2\epsilon_s$ in the limit of $qa\to 0$ and $pa=0$. This can also be seen from the expansion in Eq. (4.2), since the only nonvanishing term in this limit is the $n=0$ term.

So far we have restricted our attention to the case $\epsilon_0=\epsilon_s$. In the next section we apply the well-known mirror-image method to study the more general problem when the insulator dielectric constant ϵ_0 takes on an arbitrary value.

V. GENERAL INTERFACE

When the background dielectric constant of the insulator in the space $x>0$ is different than that of the superlattice, we must solve the complete potential equation (2.10). The term proportional to $\epsilon_s-\epsilon_0$ is complicated because it is difficult to solve for the potential $\phi(x=0,z)$ at the interface. We transform this equation into an equation for $\phi(x<0)$ by using the mirror-image technique.

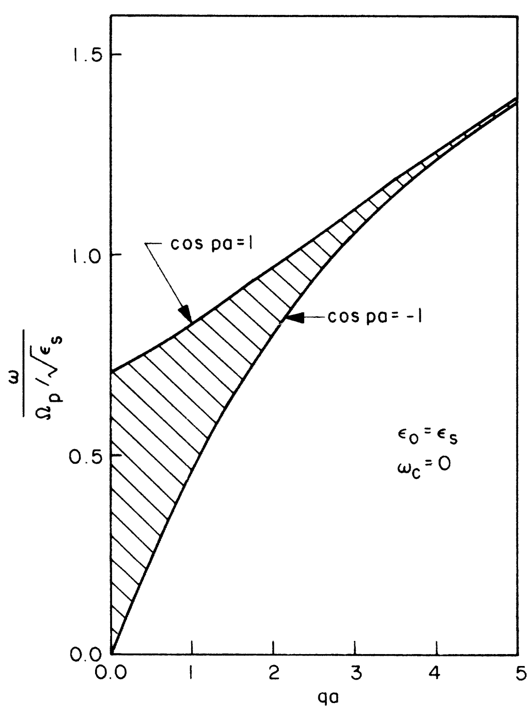

FIG. 4. Numerical dispersion relation computed from Eq. (4.14) with the same parameters as those in Fig. 2. The matrix is truncated to an order of $N=9$.

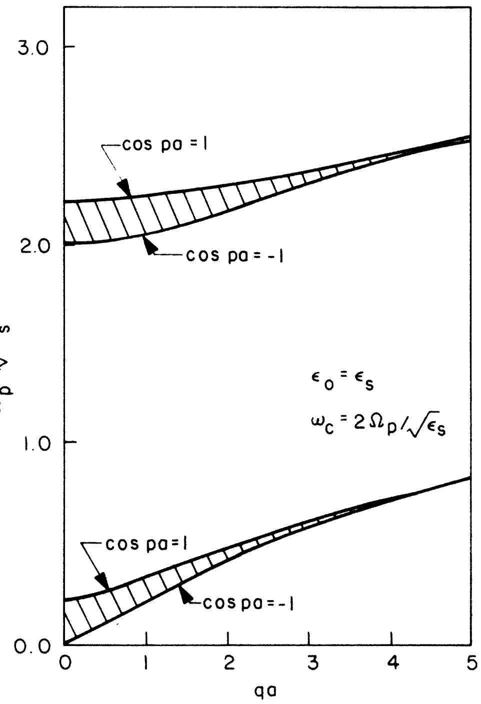

FIG. 5. Dispersion relation from numerical computation of Eq. (4.14) for the same parameters as in Fig. 3. The magnetic field is chosen such that $\omega_c = 2\Omega_p/(\epsilon_s)^{1/2}$.

As is well known from classical electrostatics, the potential in the region $x<0$ due to a point charge Q located at the coordinate $(x=-x_0<0, y=0, z=0)$ in the presence of an interface at $x=0$ can be written

$$\phi(x,y,z)=\frac{Q}{\epsilon_s}\left[[(x+x_0)^2+y^2+z^2]^{-1/2} + \frac{\epsilon_s-\epsilon_0}{\epsilon_s+\epsilon_0}[(x-x_0)^2+y^2+z^2]^{-1/2}\right].$$

The effect of different dielectric constants across the interface is equivalent to placing charge Q' at $(x_0,0,0)$ with

$$Q'=Q\frac{\epsilon_s-\epsilon_0}{\epsilon_s+\epsilon_0}.$$

This should be true for an arbitrary change distribution from the principle of superposition.

In the $l=0$ layer of the superlattice, the charge distribution in the region of $x<0$ is given in Eq. (2.14). The mirror-image charge distribution in $x>0$ is

$$\begin{aligned} n_0(x>0) &= \frac{\epsilon_s-\epsilon_0}{\epsilon_s+\epsilon_0} n_0(-x) \\ &= \frac{\epsilon_s-\epsilon_0}{\epsilon_s+\epsilon_0}\left[\frac{\sigma_{xx}}{i\omega}\left[q^2-\frac{\partial^2}{\partial x^2}\right]\phi(-x) - \frac{1}{i\omega} j_x(0^-)\delta(x)\right]. \end{aligned} \tag{5.1}$$

The potential at $x<0$ is then determined from the following integral equation:

$$\phi(x<0)=4\pi\left[\int_{-\infty}^{0} dx' L_q(x-x')n_0(x') + \int_0^\infty dx' L_q(x-x')n_0(x')\right]. \tag{5.2}$$

This is the eigenfunction for $\phi(x<0)$ and can be transformed into a matrix equation by the expansion in Eq. (4.2). This leads to a generalization of Eq. (4.4):

$$\alpha_n = \frac{4\pi\sigma_{xx}}{i\omega\epsilon_s}\sum_{n'=0}^{\infty}\alpha_{n'}\left[J_{nn'}+\frac{\epsilon_s-\epsilon_0}{\epsilon_s+\epsilon_0}K_{nn'} + \frac{2\epsilon_s}{\epsilon_s+\epsilon_0}(2n'+1\mp\omega_c/\omega)I_n\right], \tag{5.3}$$

where $J_{nn'}$ and I_n are defined in Eqs. (4.5) and (4.6). $K_{nn'}$ is defined by the relation

$$K_{nn'}=2q\int_{-\infty}^{0} dx\,\exp(qx)L_n(-2qx)\int_0^\infty dx' L_q(x-x')\left[q^2-\frac{\partial^2}{\partial(x')^2}\right][\exp(-qx')L_{n'}(2qx')]. \tag{5.4}$$

The magnetoplasmon dispersion is determined from the equation

$$\det\left\{\delta_{nn'}-D\left[S_{nn'}+\frac{\epsilon_s-\epsilon_0}{\epsilon_s+\epsilon_0}T_{nn'}+\frac{2\epsilon_s}{\epsilon_s+\epsilon_0}\left[1\mp\frac{\omega_c}{\omega}\right]F_n\right]\right\}=0, \tag{5.5}$$

with the notation being defined in Eqs. (4.10)–(4.13) and

$$T_{nn'}=\sum_{m=-\infty}\left[\left[\frac{\gamma-1}{\gamma+1}\right]^{n+1}-\left[\frac{\gamma-1}{\gamma+1}\right]^{n+n'+1}\right]\frac{1}{\gamma}. \tag{5.6}$$

Equation (5.5) is a generalization of Eq. (4.14).

The dispersion relation of the magnetoplasmon is computed for a system consisting of a GaAs-AlGaAs superlattice with its lateral surface exposed in vacuum. We choose $\epsilon_s=13.6$ and $\epsilon_0=1$. The results are plotted in Figs. 6 and 7 for $\omega_c=0$ and $\omega_c=2\Omega_p/(\epsilon_s)^{1/2}$, respectively. Comparing to the dispersion relations for $\epsilon_0=\epsilon_s$ in Figs. 4 and 5, we observe that for fixed wave vector, the plasma frequency is higher for $\epsilon_0<\epsilon_s$, and should be lower for $\epsilon_0>\epsilon_s$. This can be seen in the analytic expression $\omega(\omega\pm\omega_c)=\Omega_p^2/(\epsilon_0+\epsilon_s)$ in the limit of $qa\to0$ and $pa=0$.

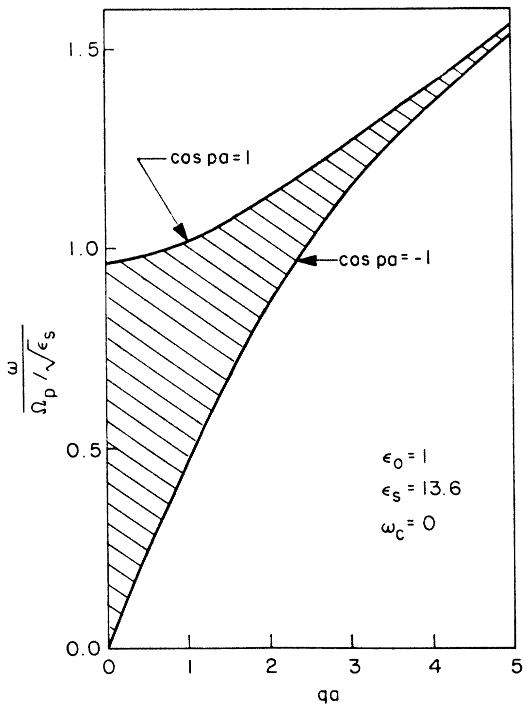

FIG. 6. Lateral surface plasma dispersion for a system of general interface in the absence of a static magnetic field. The two different background dielectric constants are $\epsilon_s = 13.6$ and $\epsilon_0 = 1$.

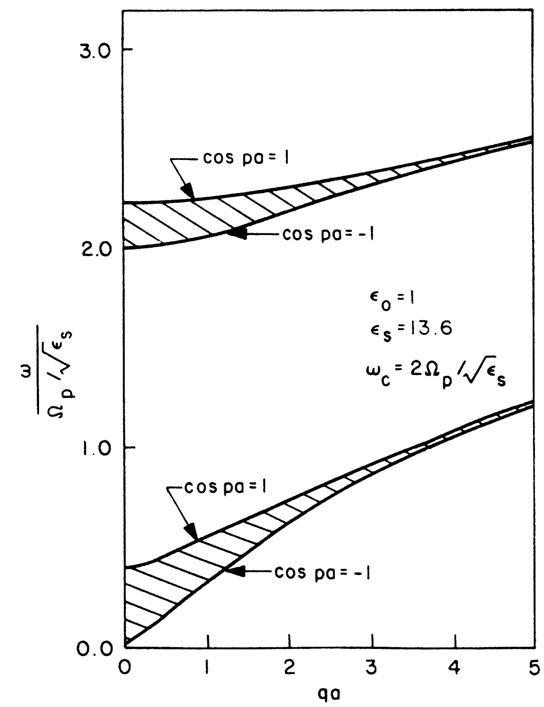

FIG. 7. Lateral surface magnetoplasma dispersion with a static magnetic field in the z direction such that $\omega_c = 2\Omega_p/(\epsilon_s)^{1/2}$. The background dielectric constants are $\epsilon_0 = 1$ and $\epsilon_s = 13.6$.

VI. CONCLUSION AND DISCUSSION

We have predicted a new type of surface magnetoplasmons which occurs on the lateral surfaces of a semiconductor superlattice. The dispersion relation of these edge collective modes has been studied when a static magnetic field of arbitrary magnitude is applied parallel to the surface. The surface excitations have several remarkable properties which might be of experimental interest. These collective excitations are free from Landau damping, since the band of excitation spectrum is well above the single-particle continuum. For small values of q and for $p \neq 0$, the modes are acoustic in nature, and the spectrum extends to arbitrarily small values of qa. This means that no minimum in-plane momentum transfer is required in the experiment. The presence of a magnetic field parallel to the interface would favor possible observation of these surface modes in the experiment because the phase velocity of the waves in the long-wavelength limit can be greatly reduced and the energy spectrum is well separated from that of the bulk excitations. The optimal choice is $\omega_c > \Omega_p/(\epsilon_s)^{1/2}$. For a GaAs-(AlGa)As superlattice, typical parameters are $\epsilon_s = 13$, $m = 0.067 m_e$, $n_s = 10^{11}$ cm^{-2}, and $a = 500$ Å. These conditions lead to $\Omega_p/(\epsilon_s)^{1/2} = 8.5 \times 10^{12}$ sec^{-1}, which corresponds to a magnetic field of 3300 G. Possible methods of observing these excitations could be attenuated total reflection, resonant Raman and Brillouin scattering, or electron-energy-loss spectroscopy.

ACKNOWLEDGMENT

This research is supported by the U.S. Army Research Office, Durham.

[1]F. Stern, Phys. Rev. Lett. **18**, 546 (1967).

[2]A. L. Fetter, Ann. Phys. (N.Y.) **81**, 367 (1973); **88**, 1 (1974).

[3]S. Das Sarma and J. J. Quinn, Phys. Rev. B **25**, 7603 (1982).

[4]W. L. Bloss, Solid State Commun. **44**, 363 (1982); W. L. Bloss and E. M. Brody, *ibid.* **43**, 523 (1982).

[5]D. Olego, A. Pinczuk, A. C. Gossard, and W. Wiegmann, Phys. Rev. B **25**, 7867 (1982).

[6]G. Gonzalez de la Cruz, A. Tselis, and J. J. Quinn, J. Phys. Chem. Solids **44**, 807 (1983); A. Tselis and J. J. Quinn, Phys. Rev. B **29**, 3318 (1984).

[7]A. Pinczuk, J. M. Worlock, H. L. Stormer, R. Dingle, W. Wiegmann, and A. C. Gossard, Solid State Commun. **36**, 43 (1980).

[8]P. Manuel, G. A. Sai-Habasz, L. L. Chang, C. A. Chang, and L. Esaki, Phys. Rev. Lett. **37**, 1701 (1976).

[9]R. Sooryakumar, A. Pinczuk, A. Gossard, and W. Wiegmann, Phys. Rev. **31**, 2578 (1985).

[10]R. Camley and D. Mills, Phys. Rev. B **29**, 1695 (1984).

[11]G. Giuliani, J. J. Quinn, and R. F. Wallis, J. Phys. (Paris) Colloq. **45**, C5-285 (1984); and unpublished.

[12]G. Giuliani and J. J. Quinn, Phys. Rev. Lett. **51**, 919 (1983); G. Qin, G. Giuliani, and J. J. Quinn, Phys. Rev. B **28**, 6144 (1983).
[13]J. K. Jain and P. B. Allen, Phys. Rev. Lett. **54**, 947 (1985).
[14]P. Hawrylak, J.-W. Wu, and J. J. Quinn, Phys. Rev. B **31**, 7855 (1985).
[15]J.-W. Wu, P. Hawrylak, and J. J. Quinn, Phys. Rev. Lett. **55**, 879 (1985).
[16]D. B. Mast, A. J. Dahm, and A. L. Fetter, Phys. Rev. Lett. **54**, 1706 (1985).
[17]See, for example, G. F. Carrier, M. Krook, and C. E. Pearson, *Functions of a Complex Variable* (McGraw-Hill, New York, 1966), Secs. 8-1, 8-3, and 8-4.
[18]K. W. Chiu and J. J. Quinn, Nuovo Cimento **10**, 1 (1972); Phys. Rev. B **5**, 4707 (1972).